

## Scaling Theory of the Anderson Transition in Random Graphs: Ergodicity and Universality

I. García-Mata,<sup>1,2</sup> O. Giraud,<sup>3</sup> B. Georgeot,<sup>4</sup> J. Martin,<sup>5</sup> R. Dubertrand,<sup>5</sup> and G. Lemarié<sup>4,\*</sup>

<sup>1</sup>*Instituto de Investigaciones Físicas de Mar del Plata (IFIMAR), CONICET–UNMdP, Funes 3350, B7602AYL Mar del Plata, Argentina*

<sup>2</sup>*Consejo Nacional de Investigaciones Científicas y Tecnológicas (CONICET), Godoy Cruz 2290 (C1425FQB) CABA, Argentina*

<sup>3</sup>*LPTMS, CNRS, Univ. Paris-Sud, Université Paris-Saclay, 91405 Orsay, France*

<sup>4</sup>*Laboratoire de Physique Théorique, IRSAMC, Université de Toulouse, CNRS, UPS, 31062 Toulouse, France*

<sup>5</sup>*Institut de Physique Nucléaire, Atomique et de Spectroscopie, CESAM, Université de Liège, Bât. B15, B–4000 Liège, Belgium*

(Received 9 September 2016; published 17 April 2017)

We study the Anderson transition on a generic model of random graphs with a tunable branching parameter  $1 < K < 2$ , through large scale numerical simulations and finite-size scaling analysis. We find that a single transition separates a localized phase from an unusual delocalized phase that is ergodic at large scales but strongly nonergodic at smaller scales. In the critical regime, multifractal wave functions are located on a few branches of the graph. Different scaling laws apply on both sides of the transition: a scaling with the linear size of the system on the localized side, and an unusual volumic scaling on the delocalized side. The critical scalings and exponents are independent of the branching parameter, which strongly supports the universality of our results.

DOI: 10.1103/PhysRevLett.118.166801

Ergodicity properties of quantum states are crucial to assess transport properties and thermalization processes. They are at the heart of the eigenstate thermalization hypothesis that has attracted enormous attention lately [1]. A paramount example of nonergodicity is Anderson localization where the interplay between disorder and interference leads to exponentially localized states [2]. In 3D, a critical value of disorder separates a localized phase from an ergodic delocalized phase. At the critical point eigenfunctions are multifractal, another nontrivial example of nonergodicity [3,4]. Recently, those questions have been particularly highlighted in the problem of many-body localization [5–9]. Because Fock space has locally a treelike structure, the problem of Anderson localization on different types of graphs [10–15] has attracted renewed activity [16–26]. In particular, the existence of a delocalized phase with nonergodic (multifractal) eigenfunctions lying on an algebraically vanishing fraction of the system sites is debated [19–21,25,26].

The problem of nonergodicity also arises in another context corresponding to glassy physics [27]. For directed polymers on the Bethe lattice [28], a glass transition leads to a phase where a few branches are explored among the exponential number available. As there is a mapping to directed polymer models in the Anderson-localized phase [10,29–31], it has been recently proposed that this type of nonergodicity (where the volume occupied by the states scales logarithmically with system volume) could also be relevant in the delocalized phase [18]. Note however that it has been envisioned that this picture could be valid only up to a finite but very large length scale [32] so that the analogy with the usual physics of directed polymers may not be relevant in the delocalized phase.

In this Letter, we study the Anderson transition (AT) in a family of random graphs [33–35], where a tunable parameter  $p$  allows us to interpolate continuously between the 1D Anderson model and the random regular graph model of infinite dimensionality. Our main tool is the single parameter scaling theory of localization [36]. It has been used as a crucial tool to interpret the numerical simulations of Anderson localization in finite dimensions [3,37–39] and to achieve the first experimental measurement of the critical exponent of the AT in 3D [40]. In our case, the infinite dimensionality of the graphs leads to highly nontrivial finite-size scaling properties: unusually, we find different scaling laws on each side of the transition. Our detailed analysis of extensive numerical simulations leads to the following scenario. A single AT separates a localized phase from an ergodic delocalized phase. However, a characteristic nonergodicity volume (NEV)  $\Lambda$  emerges in the latter phase. For scales below  $\Lambda$ , states are nonergodic in the sense that they take significant values only on a few branches, on which they additionally display multifractal fluctuations. For scales above  $\Lambda$ , this structure repeats itself and leads to large scale ergodicity. At the threshold,  $\Lambda$  diverges, and the behavior below  $\Lambda$  extends to the whole system. The critical behaviors do not depend on the graph parameter  $p$ , which strongly supports the universality of this scenario.

We use two complementary approaches to describe localization properties. First, we derive recursive equations for the local Green function using a mapping to a tree [10], which we solve using the pool method from glassy physics [16,29], and analyze the critical behavior by finite-size scaling. Second, we perform exact diagonalization of very large system sizes, and extract the scaling properties of

eigenfunction moments. We use the box-counting method in this new context of graphs of infinite dimensionality to perform a local analysis and to extract the NEV  $\Lambda$  unambiguously.

*Random graph model.*—We consider a 1D lattice of  $N$  sites with periodic boundary conditions. Each site is connected to its nearest neighbors and  $\lfloor pN \rfloor$  shortcut links are added ( $\lfloor \cdot \rfloor$  is the integer part). These shortcuts give an average distance between pairs of sites increasing logarithmically with  $N$ , so that the graph has infinite dimensionality [41,42]. The system is described by the Hamiltonian  $H = \sum_{i=1}^N \varepsilon_i |i\rangle\langle i| + \sum_{\langle i,j \rangle} |i\rangle\langle j| + \sum_{k=1}^{\lfloor pN \rfloor} (|i_k\rangle\langle j_k| + |j_k\rangle\langle i_k|)$  in position basis  $\{|i\rangle, 1 \leq i \leq N\}$ . The first term describes on-site disorder with  $\varepsilon_i$  independent and identically distributed Gaussian random variables with zero mean and standard deviation  $W$ . The second term runs over nearest neighbors. The third term gives the long-range links that connect pairs  $(i_k, j_k)$ , randomly chosen with  $|i_k - j_k| > 1$ .  $p = 0$  is the 1D Anderson model. At finite  $p$ , our system is a random graph with mean connectivity  $K = 1 + 2p$ , giving access to the regime  $1 < K \leq 2$ .

*Glassy physics approach.*—We first use a recursive technique used to investigate localization on the Bethe lattice [10,16,28,29,45]. It is exact for a Cayley tree (which has no loop), but only an approximation for a generic graph. For a regular tree with  $K + 1$  neighbors, the diagonal elements  $G_{ii}$  of the Green operator follow  $G_{ii} = (\varepsilon_i - E - \sum_{j=1}^K G_{jj})^{-1}$ , where the sum is over the  $K$  children  $j$  of node  $i$  [10]. In our model, each parent node has either one or two children. This leads to three recursion equations determining the probability distribution of  $G$  [42].

To probe localization properties, we use the belief propagation method (or pool method), which consists of sampling the distribution of  $G$  with a Monte Carlo approach [16,29]. For a fixed value of  $E$ , we start from an initial pool of  $M_{\text{pool}}$  complex values for the local variables  $G_{ii}$ ,  $1 \leq i \leq M_{\text{pool}}$ , and calculate the next generation by applying the recursion relations. The important quantity is the typical value of the imaginary part  $\text{Im}G$ , which goes to zero in the localized phase as  $\langle \ln \text{Im}G \rangle \sim -M_g/\xi_l$  when the number of generations  $M_g$  tends to infinity, ( $\langle X \rangle$  denotes ensemble averaging) whereas in the delocalized phase  $\langle \ln \text{Im}G \rangle$  converges to a finite value. We observed that the localization length  $\xi_l$  diverges at the transition as  $\xi_l \sim [W - W_c(M_{\text{pool}})]^{-\nu_l}$  with the critical exponent  $\nu_l \approx 1$  and a critical disorder  $W_c(M_{\text{pool}})$  that depends on  $M_{\text{pool}}$  (see also Refs. [16,29]). We determined  $W_c(M_{\text{pool}})$  for values of  $M_{\text{pool}}$  up to  $10^6$ . The results, presented in the inset of Fig. 1, show that  $W_c(M_{\text{pool}})$  converges to  $W_c^\infty \approx 1.77$  for  $p = 0.06$  as  $M_{\text{pool}} \rightarrow \infty$ .

Following Refs. [16,46], we assume that  $\langle \ln \text{Im}G \rangle$  follows a single parameter scaling law:

$$\langle \ln \text{Im}G \rangle = -(M_g)^\rho \mathcal{F}_G(M_g/\xi) \quad (1)$$

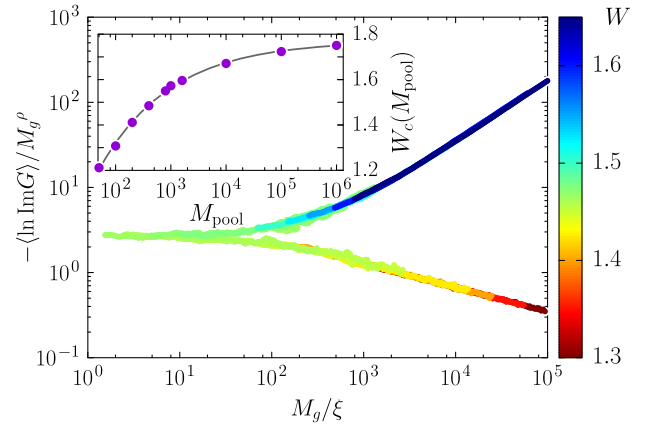


FIG. 1. Single parameter scaling of  $\langle \ln \text{Im}G \rangle$  versus number of generations  $M_g$ , for  $M_{\text{pool}} = 400$ ,  $M_g$  from  $2M_{\text{pool}}$  to  $10^5$ ,  $p = 0.06$ , and  $W \in [1.3, 1.65]$  (see color code).  $\langle \ln \text{Im}G \rangle \sim -M_g^\rho$  with  $\rho \approx 0.28$  at  $W = 1.46 \approx W_c(M_{\text{pool}})$ . Finite-size scaling of  $-\langle \ln \text{Im}G \rangle / M_g^\rho$  following Eq. (1). The scaling parameter  $\xi$  diverges at the threshold as  $\xi \sim |W - W_c(M_{\text{pool}})|^{-\nu}$  with  $\nu \approx 1.4$  and  $W_c(M_{\text{pool}}) \approx 1.46$ . Inset: critical disorder  $W_c(M_{\text{pool}})$  versus  $M_{\text{pool}}$ . The line is a fit by  $W_c(M_{\text{pool}}) = W_c^\infty + A_0 M_{\text{pool}}^{-\beta}$  with  $A_0$  a constant,  $W_c^\infty = 1.77$ , and  $\beta = 0.33$ . The error bars are of the same order as the fluctuations of the data points.

with the scaling parameter  $\xi \sim |W - W_c(M_{\text{pool}})|^{-\nu}$  [47]. To correctly sample the distribution of  $\text{Im}G$ , values of  $M_{\text{pool}}$  as large as possible are usually considered, with typically  $M_g \leq M_{\text{pool}}$  (see above). However, our numerical results show that the scaling behavior (1) is visible only for  $M_g \gg M_{\text{pool}}$ . Moreover, for a given initial pool, the fluctuations of  $\langle \ln \text{Im}G \rangle$  when  $M_g$  is varied can be extremely large (especially at criticality). In order to analyze the scaling behavior (1) we therefore considered values of  $M_{\text{pool}}$  from 50 to 800, and  $M_g$  from  $2M_{\text{pool}}$  to  $10^5$ , and averaged additionally over 100 different realizations of the pool. The scaling hypothesis (1) is confirmed by the data collapse shown in Fig. 1, allowing us to extract the scaling exponents  $\nu \approx 1.4 \pm 0.2$  and  $\rho \approx 0.28 \pm 0.07$ , which do not depend on  $M_{\text{pool}}$ . Therefore, in the delocalized phase, the typical value of  $\text{Im}G$  vanishes at the transition with an essential singularity  $\lim_{M_g \rightarrow \infty} \langle \ln \text{Im}G \rangle \sim -(W_c(M_{\text{pool}}) - W)^{-\kappa}$  with  $\kappa = \rho\nu \approx 0.39 \pm 0.16$  the critical exponent in the delocalized phase, compatible with the value  $1/2$  predicted analytically [14,15]. Moreover, from  $\nu_l = \nu(1 - \rho)$  we recover the value  $\nu_l \approx 1.0 \pm 0.2$  (see also Ref. [16]).

*Scaling analysis of eigenfunction moments.*—We now describe the results of our second approach. We performed exact diagonalizations of many realizations of graphs with up to  $N \sim 2 \times 10^6$  sites and obtained for each realization 16 eigenfunctions at the band center using the Jacobi-Davidson method [48]. We performed a multifractal analysis of the eigenfunctions  $|\psi\rangle$  by considering the scaling of average moments  $\langle P_q \rangle = \langle \sum_{i=1}^N |\psi_i|^{2q} \rangle$  for real  $q$  as a

function of  $N$ . For a  $d$ -dimensional system of linear size  $L$  and volume  $N = L^d$ , multifractal eigenfunctions have  $\langle P_q \rangle \sim L^{-\tau_q}$  at large  $L$ , or equivalently  $\langle P_q \rangle \sim N^{-\chi_q}$  with  $\chi_q = \tau_q/d$ , defining nontrivial multifractal dimensions  $D_q = \tau_q/(q-1)$ . In the localized case  $D_q = 0$  whereas for wave functions delocalized over the whole space  $D_q = d$ . Our graphs however have infinite dimensionality [49], with system volume  $N = V_g(d_N)$  exponential in the linear size  $d_N \sim \log_2 N$ , the diameter of the system [42]. Figure 2 shows that a critical behavior  $\langle P_2 \rangle \sim (\log_2 N)^{-\tau_2} \sim d_N^{-\tau_2}$  actually holds with  $\tau_2 \approx 0.42$  for  $p = 0.06$  and  $W = 1.6 \approx W_c$  (upper right inset). This  $d_N^{-\tau_q}$  dependence entails that a behavior  $\langle P_q \rangle \sim N^{-\chi_q}$  would lead to  $\chi_q = 0$ , in line with the analytical predictions [4,13,15] at infinite dimensionality. Moreover, in analogy with directed polymers, in the localized phase eigenfunctions are located on a few branches of the graph on which they are exponentially localized. At criticality the localization length diverges to the system size  $d_N$  and one should observe critical wave functions located on a few branches on which they display additional multifractal fluctuations.

The following one-parameter scaling hypothesis should naturally follow:

$$\langle P_q \rangle = d_N^{-\tau_q} \mathcal{F}_{\text{lin}}(d_N/\xi). \quad (2)$$

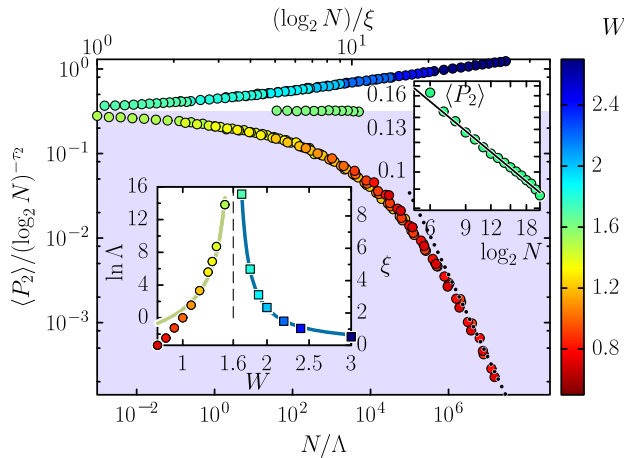


FIG. 2. Scaling of moments  $\langle P_2 \rangle$  with  $N$  for  $p = 0.06$  and  $W \in [0.7, 3]$ . For  $W > W_c$  (localized phase), linear scaling of  $\langle P_2 \rangle / (\log_2 N)^{-\tau_2}$  following Eq. (2) with  $\tau_2 = 0.42$ . For  $W < W_c$  (delocalized phase), volumic scaling following Eq. (3). Data for  $W = W_c$  have been shifted horizontally for visibility. Dotted line shows asymptotic ergodic behavior  $N^{-1}(\log_2 N)^{\tau_2}$  corresponding to  $\langle P_2 \rangle \sim N^{-1}$ . Upper inset (note the log scale): the critical behavior of  $\langle P_2 \rangle$  at  $W = 1.6 \approx W_c$  is very well fitted (black line) by  $\langle P_2 \rangle = A_0(\log_2 N)^{-\tau_2}$  with  $A_0$  a constant and  $\tau_2 \approx 0.42$ . Lower inset: correlation volume  $\Lambda$  (circles) and localization length  $\xi$  (squares) on both sides of the transition. Solid lines are the fits:  $\ln \Lambda = A_1 + A_2(W_c - W)^{-\kappa}$  (for  $W \in [1, 1.5]$ ) and  $\xi = A_3(W - W_c)^{-\nu_l}$  with  $W_c = 1.6$  and  $\kappa = 0.5$  (assigned values), yielding  $\nu_l \approx 1$ . Error bars on  $\langle P_2 \rangle$  are below the symbol size, and not taken into account in the scaling analysis.

It is consistent with the scaling theory for both the AT in finite dimension [50] and the glassy physics approach above. A careful finite-size scaling analysis of our data shows that Eq. (2) yields a very good data collapse on the localized side of the transition, see Fig. 2, upper branch in the main panel. The scaling parameter  $\xi \sim \xi_l$ , with  $\xi_l$  the localization length, diverges as  $\xi \propto (W - W_c)^{-\nu_l}$  near the AT, with  $\nu_l \approx 1$  (in agreement with the value found by our glassy physics approach).

However, in the delocalized phase, small but systematic deviations are observed [42]. This leads us to propose a scaling hypothesis in this phase different from Eq. (2); the system volume  $N$  could instead be rescaled by a characteristic volume  $\Lambda$ :

$$\langle P_q \rangle = d_N^{-\tau_q} \mathcal{F}_{\text{vol}}(N/\Lambda). \quad (3)$$

Scaling hypotheses (2) and (3) are strictly equivalent in finite dimension, but lead to very different behaviors for infinite dimensionality. In the linear scaling (2), delocalized states consist of the repetition of linear critical structures of size  $\xi$  and moments behave as  $\langle P_q \rangle \approx \xi^{-\tau_q} N^{-(q-1)/\xi}$ . It is reminiscent of the nonergodic behavior discussed in Refs. [19–21,25]. In the volumic scaling (3), delocalized states consist of  $N/\Lambda$  volumic critical structures of size  $\Lambda$ , and moments behave as  $\langle P_q \rangle \approx (\Lambda/N)^{q-1} [1 - \tau_q(\xi/d_N)]$  [42]. This is consistent with previous analytical results [14,15]. The finite-size scaling shown in Fig. 2 clearly indicates that the volumic scaling (3) puts all the curves onto a single scaling function in the delocalized phase,  $W < W_c$ , with the correlation volume diverging exponentially at the transition as  $\ln \Lambda \approx (W_c - W)^{-\kappa}$ ,  $\kappa \approx 0.5$  (in good agreement with our glassy physics approach, the analytical prediction  $\kappa = 1/2$  [14,15], and the recent numerical results [22]).

*Nonergodicity volume.*—To probe the local properties of localization, we use the box-counting method, which consists of investigating the scaling properties of moments of coarse-grained wave functions. Dividing the system of  $N$  sites into boxes of  $\ell$  consecutive sites along the lattice (i.e., not following the long-range links) and defining a measure  $\mu_k = \sum_{i \in \text{box } k} |\psi_i|^2$  of each box, moments are defined as  $P_q(\ell) = \sum_k \mu_k^q$ . For multifractal states, they scale as  $\langle P_q(\ell) \rangle \sim \ell^{\pi_q}$  at large  $N$  with nontrivial  $\pi_q$  [51].  $\pi_q = 0$  for localized states, and  $\pi_q = q - 1$  for completely delocalized states. Figure 3 displays the moments  $\langle P_2(\ell) \rangle$  versus  $\ell$  for different  $W$ , and shows that three distinct regimes can be identified. At scales below the mean distance  $1/(2p)$  between two long-range links, moments have a power-law behavior with  $\pi_2 \approx 0.5 \pm 0.1$ , in the vicinity of  $W_c$  where  $\xi \gg 1/(2p)$ . For  $\ell \leq 1/(2p)$ , only one branch is probed and the value of  $\pi_2$  should measure the critical multifractality on a few branches.  $\pi_2$  is indeed close to  $\tau_2 \approx 0.42$  found above. At intermediate scales, moments follow a plateau characteristic of a strongly

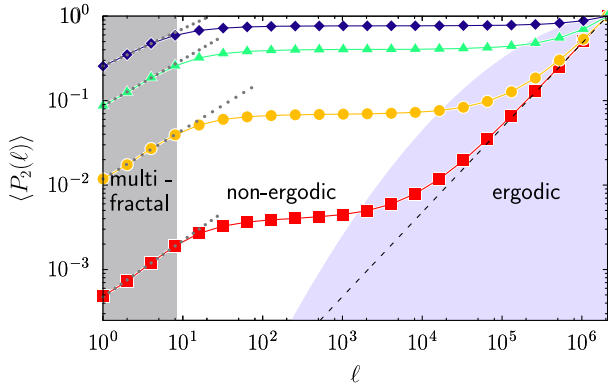


FIG. 3.  $\langle P_2 \rangle$  versus box volume  $\ell$  for  $N = 2^{21}$  with  $p = 0.06$  and  $W = 1.0$  (square), 1.3 (circle), 1.6 (triangle), 2.4 (diamond). The gray shaded area on the left delimits the small  $\ell < 1/2p$  multifractal behavior (the dotted lines have a slope ranging from 0.44 to 0.66). The light-blue shaded area on the right delimits the large scale  $\ell \gg \lambda$  ergodic behavior (the dashed line has slope 1).

nonergodic behavior. This corresponds to the critical behavior we observe when changing  $N$ , i.e.,  $\langle P_2 \rangle \sim (\log_2 N)^{-\tau_2}$ ; thus,  $\langle P_2 \rangle \sim N^{-\chi_2}$  with  $\chi_2 = 0$  (see Fig. 2 and Fig. S4 of Ref. [42]). Beyond a characteristic scale  $\lambda$  that depends on  $W$  and  $N$ , moments are linear in  $\ell$ , which corresponds to an ergodic behavior. In the localized case  $\lambda \sim N$ , so that there is no ergodic behavior, while in the delocalized case,  $\lambda$  saturates to a finite value (see below), and states are ergodic at scales above  $\lambda$ , and nonergodic below; we therefore call  $\lambda$  the NEV. One can extract  $\lambda$  from a rescaling of the local slopes  $\tilde{\pi}_q(\ell) \equiv (d \ln \langle P_q(\ell) \rangle) / (d \ln \ell)$  [51] in the ergodic regime  $\ell \gg \lambda$  (see inset of Fig. 4).

The data shown in Fig. 4 can be described by a linear scaling  $\lambda / (N / \log_2 N) = \mathcal{G}_{\text{lin}}(\log_2 N / \xi)$  in the localized regime, with  $\xi \sim \xi_l$  the localization length, and by a volumic scaling  $\lambda / (N / \log_2 N) = \mathcal{G}_{\text{vol}}(N / \Lambda)$  in the delocalized regime. The behavior at the threshold  $\lambda \sim N / \log_2 N$  shows that critical states are located on a few branches of  $\log_2 N$  sites. This confirms that critical states have multifractal fluctuations on a logarithmically small fraction of the system volume. Moreover, the volumic scaling shows that in the limit  $N \gg \Lambda$  the NEV  $\lambda$  saturates to the correlation volume  $\Lambda$  [42]. This implies that the delocalized phase is ergodic in the limit of large  $N \gg \Lambda$ .

We have checked that the scaling properties are the same for  $q \geq 1$  whereas for  $q < 1$  the volumic behavior of the delocalized phase extends to the critical and localized regimes. This is to be expected [15,17]: for  $q < 1$  all small values of the wave function, even outside the few localization branches, contribute to the moment.

**Universality.**—We have considered different values of the graph parameter from  $p = 0.01$  to  $p = 0.49$  [42], changing the average branching parameter  $K = 1 + 2p$  from  $K = 1.02$  to  $K = 1.98$ . Our data show that the critical scalings are insensitive to  $p$ . Moreover, the critical exponents have universal values  $\kappa \approx 0.5$  and  $\nu_l \approx 1$ .

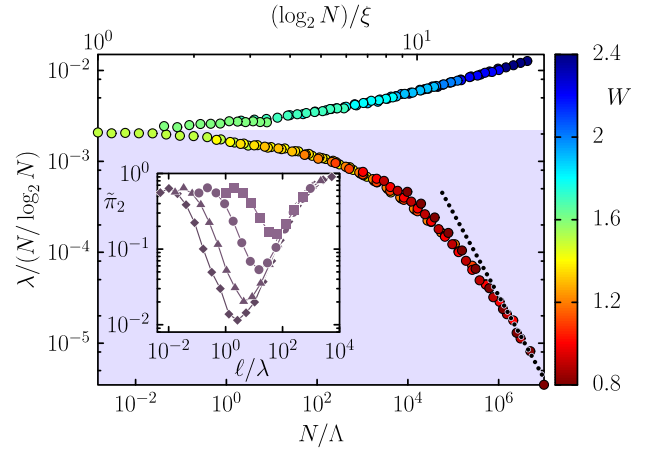


FIG. 4. Scaling behavior of the NEV  $\lambda$  with  $N = 2^{10}$  to  $2^{21}$ ,  $p = 0.06$ , and  $W \in [0.8, 2.4]$ . At the threshold  $W = W_c \approx 1.6$ ,  $\lambda \sim N / \log_2 N$ . In the localized phase, the data collapse is excellent when plotted as a function of  $(\log_2 N) / \xi$  (linear scaling, see text). In the delocalized phase, a volumic scaling as function of  $N / \Lambda$  makes the curves collapse. The dotted line shows asymptotic ergodic behavior  $N^{-1}(\log_2 N)$  corresponding to  $\lambda = \Lambda$  [42]. Inset: determination of the NEV  $\lambda$  through rescaling of  $\tilde{\pi}_2(\ell)$  data (see text) versus  $\ell / \lambda$ , in the large scale  $\ell \gg \lambda$  ergodic regime, for  $W = 1.6$  and  $N = 2^{10}$  (square),  $2^{14}$  (circle),  $2^{18}$  (triangle), and  $2^{21}$  (diamond).

**Conclusion.**—Our study strongly supports the following picture. A single transition separates a localized phase from an ergodic delocalized phase. In the delocalized phase, the NEV  $\Lambda$  separates a nonergodic behavior reminiscent of glassy physics at small scales from an ergodic behavior at large scales. At the transition,  $\Lambda$  diverges, so that the behavior below  $\Lambda$  extends to the whole system. This highlights a new type of strong nonergodicity with states located on a few branches on which they display additional multifractal fluctuations. The ergodic character of the delocalized phase is controlled by the unusual volumic scaling in this phase, different from the linear scaling that applies in the localized phase and to the whole transition in the Cayley tree as found in our glassy physics approach. Therefore, the absence of a boundary may change the nature of the AT, as envisioned in Ref. [26].

Our results apply to random graphs with  $1 < K < 2$ . In particular, for  $K = 1.98$ , we found results in agreement with the case  $K = 2$  investigated in Refs. [14,15,22,32]. Recent results [21,52] suggest that a nonergodic delocalized phase could still arise at large  $K$  (see however Ref. [23]). It will thus be very interesting to investigate this regime  $K \gg 2$  with our approach. Last, nonergodicity is usually linked with a specific dynamics, such as anomalous diffusion, which will be instructive to study. Another fascinating perspective would be to probe if our nontrivial scaling theory applies to many-body localization.

We thank Claudio Castellani and Nicolas Laflorencie for interesting discussions. We thank Calcul en Midi-Pyrénées

(CalMiP) for access to its supercomputer and the Consortium des Équipements de Calcul Intensif (CÉCI), funded by the Fonds de la Recherche Scientifique de Belgique (F. R. S.-FNRS) under Grant No. 2.5020.11. This work was supported by Programme Investissements d'Avenir under the program ANR-11-IDEX-0002-02, reference ANR-10-LABX-0037-NEXT, by Agence Nationale de la Recherche (ANR) Grant K-BEC No. ANR-13-BS04-0001-01, by Actions de Recherche Concertées (ARC) Grant No. QUANDROPS 12/17-02, and by the Consejo Nacional de Investigaciones Científicas y Técnicas (CONICET) - Centre National de la Recherche Scientifique (CNRS) bilateral Project No. PICS06303R.

\*Corresponding author.

lemaire@irsamc.ups-tlse.fr

- [1] R. V. Jensen and R. Shankar, *Phys. Rev. Lett.* **54**, 1879 (1985); J. M. Deutsch, *Phys. Rev. A* **43**, 2046 (1991); M. Srednicki, *Phys. Rev. E* **50**, 888 (1994); P. Calabrese and J. Cardy, *Phys. Rev. Lett.* **96**, 136801 (2006); M. Rigol, V. Dunjko, and M. Olshanii, *Nature (London)* **452**, 854 (2008).
- [2] P. W. Anderson, *Phys. Rev.* **109**, 1492 (1958).
- [3] E. Abrahams, *50 Years of Anderson Localization* (World Scientific, Singapore, 2010), Vol. 24.
- [4] F. Evers and A. D. Mirlin, *Rev. Mod. Phys.* **80**, 1355 (2008).
- [5] P. Jacquod and D. L. Shepelyansky, *Phys. Rev. Lett.* **79**, 1837 (1997).
- [6] D. Basko, I. Aleiner, and B. Altshuler, *Ann. Phys. (Amsterdam)* **321**, 1126 (2006).
- [7] A. Pal and D. A. Huse, *Phys. Rev. B* **82**, 174411 (2010).
- [8] R. Nandkishore and D. A. Huse, *Annu. Rev. Condens. Matter Phys.* **6**, 15 (2015).
- [9] E. Altman and R. Vosk, *Annu. Rev. Condens. Matter Phys.* **6**, 383 (2015).
- [10] R. Abou-Chacra, D. Thouless, and P. Anderson, *J. Phys. C* **6**, 1734 (1973).
- [11] K. B. Efetov, *Sov. Phys. JETP* **61**, 606 (1985).
- [12] M. R. Zirnbauer, *Phys. Rev. B* **34**, 6394 (1986); *Nucl. Phys. B* **265**, 375 (1986).
- [13] C. Castellani, C. Di Castro, and L. Peliti, *J. Phys. A* **19**, L1099 (1986).
- [14] A. D. Mirlin and Y. V. Fyodorov, *J. Phys. A* **24**, 2273 (1991); Y. V. Fyodorov and A. D. Mirlin, *Phys. Rev. Lett.* **67**, 2049 (1991); A. D. Mirlin and Y. V. Fyodorov, *J. Phys. I (France)* **4**, 655 (1994).
- [15] A. D. Mirlin and Y. V. Fyodorov, *Phys. Rev. Lett.* **72**, 526 (1994).
- [16] C. Monthus and T. Garel, *J. Phys. A* **42**, 075002 (2009).
- [17] C. Monthus and T. Garel, *J. Phys. A* **44**, 145001 (2011).
- [18] G. Biroli, A. Ribeiro-Teixeira, and M. Tarzia, *arXiv*: 1211.7334.
- [19] A. De Luca, B. L. Altshuler, V. E. Kravtsov, and A. Scardicchio, *Phys. Rev. Lett.* **113**, 046806 (2014).
- [20] V. Kravtsov, I. Khaymovich, E. Cuevas, and M. Amini, *New J. Phys.* **17**, 122002 (2015).
- [21] B. Altshuler, E. Cuevas, L. Ioffe, and V. Kravtsov, *Phys. Rev. Lett.* **117**, 156601 (2016).
- [22] K. Tikhonov, A. Mirlin, and M. Skvortsov, *Phys. Rev. B* **94**, 220203 (2016).
- [23] E. Tarquini, G. Biroli, and M. Tarzia, *Phys. Rev. Lett.* **116**, 010601 (2016).
- [24] C. Monthus, *J. Stat. Mech.* (2016) 093304.
- [25] D. Facoetti, P. Vivo, and G. Biroli, *Europhys. Lett.* **115**, 47003 (2016).
- [26] K. Tikhonov and A. Mirlin, *Phys. Rev. B* **94**, 184203 (2016).
- [27] M. Mézard, G. Parisi, and M.-A. Virasoro, *Spin Glass Theory and Beyond*. (World Scientific Publishing Co., Inc., Pergamon Press, Singapore, 1990).
- [28] B. Derrida and H. Spohn, *J. Stat. Phys.* **51**, 817 (1988).
- [29] J. D. Miller and B. Derrida, *J. Stat. Phys.* **75**, 357 (1994).
- [30] A. M. Somoza, M. Ortuno, and J. Prior, *Phys. Rev. Lett.* **99**, 116602 (2007).
- [31] C. Monthus and T. Garel, *Phys. Rev. B* **80**, 024203 (2009).
- [32] G. Biroli (private communication).
- [33] C.-P. Z. Zhu and S.-J. Xiong, *Phys. Rev. B* **62**, 14780 (2000).
- [34] C.-P. Z. Zhu and S.-J. Xiong, *Phys. Rev. B* **63**, 193405 (2001).
- [35] O. Giraud, B. Georgeot, and D. L. Shepelyansky, *Phys. Rev. E* **72**, 036203 (2005).
- [36] E. Abrahams, P. W. Anderson, D. C. Licciardello, and T. V. Ramakrishnan, *Phys. Rev. Lett.* **42**, 673 (1979).
- [37] J. Pichard and G. Sarma, *J. Phys. C* **14**, L127 (1981).
- [38] A. MacKinnon and B. Kramer, *Phys. Rev. Lett.* **47**, 1546 (1981).
- [39] K. Slevin and T. Ohtsuki, *Phys. Rev. Lett.* **82**, 382 (1999).
- [40] J. Chabé, G. Lemarié, B. Grémaud, D. Delande, P. Szriftgiser, and J. C. Garreau, *Phys. Rev. Lett.* **101**, 255702 (2008).
- [41] D. J. Watts and S. H. Strogatz, *Nature (London)* **393**, 440 (1998).
- [42] See Supplemental Material at <http://link.aps.org/supplemental/10.1103/PhysRevLett.118.166801> for more information about the topological properties of the random graphs considered, the recursion equations used in the glassy physics approach, and the scaling analysis performed in this work, which includes Refs. [43,44].
- [43] B. Bollobás and W. Fernandez de la Vega, *Combinatorica* **2**, 125 (1982).
- [44] E. Bogomolny and O. Giraud, *Phys. Rev. E* **88**, 062811 (2013).
- [45] M. V. Feigelman, L. B. Ioffe, and M. Mézard, *Phys. Rev. B* **82**, 184534 (2010).
- [46] B. Derrida and D. Simon, *Europhys. Lett.* **78**, 60006 (2007).
- [47] Note that in the scaling law (1), the scaling parameter  $\xi$  is to be distinguished from the localization length  $\xi_l$ . In particular, they have different critical exponents  $\nu$  and  $\nu_l$ , respectively (see also Ref. [16]).
- [48] M. Bollhöfer and Y. Notay, *Comput. Phys. Commun.* **177**, 951 (2007).
- [49] S. Dorogovtsev, *Lectures on Complex Networks* (Oxford University Press, New York, 2010).
- [50] A. Rodriguez, L. J. Vasquez, K. Slevin, and R. A. Römer, *Phys. Rev. B* **84**, 134209 (2011).
- [51] R. Dubertrand, I. García-Mata, B. Georgeot, O. Giraud, G. Lemarié, and J. Martin, *Phys. Rev. Lett.* **112**, 234101 (2014); *Phys. Rev. E* **92**, 032914 (2015).
- [52] B. L. Altshuler, L. B. Ioffe, and V. E. Kravtsov, *arXiv*: 1610.00758.